On-site CT-derived cFFR in patients with suspected coronary artery disease: Feasibility on a 128-row CT scanner in everyday clinical practice

Nicht-invasive Vor-Ort-Quantifizierung der cFFR bei Patienten mit Verdacht auf koronare Herzkrankheit: Durchführbarkeit auf einem 128-Zeilen CT-Scanner im klinischen Alltag

Authors

Theresia Baumeister[1], Christopher Kloth[1], Stefan Andreas Schmidt[1], Steffen Kloempken[1], Horst Brunner[1], Dominik Buckert[2], Peter Bernhardt[3], Christoph Panknin[4], Meinrad Beer[1]

Affiliations

1 Department of Diagnostic and Interventional Radiology, Ulm University Hospital, Ulm, Germany
2 Department of Internal Medicine II, Ulm University Hospital, Ulm, Germany
3 Heart Clinic Ulm, Herzklinik Ulm Dr. Haerer und Partner, Ulm, Germany
4 Scientific Collaborations Siemens Healthcare GmbH, Erlangen, Germany

Key words

CT, CT-angiography, cardiac

received 27.11.2022
accepted 11.07.2023
published online 11.10.2023

Bibliography

Fortschr Röntgenstr 2024; 196: 62–71
DOI 10.1055/a-2142-1643
ISSN 1438-9029

Georg Thieme Verlag KG, Rüdigerstraße 14,
70469 Stuttgart, Germany

Correspondence

Dr. Christopher Kloth
Abteilung für Diagnostische und Interventionelle Radiologie, Universitätsklinikum Ulm, Albert-EInstein-Allee 23,
89070 Ulm, Germany
christopher.kloth@uniklinik-ulm.de

Additional material is available at
https://doi.org/10.1055/a-2142-1643

ABSTRACT

Purpose Technical feasibility of CT-based calculation of fractional flow reserve (cFFR) using a 128-row computed tomography scanner in an everyday routine setting. Post-processing and everyday practicability should be analyzed on the scanner on-site in connection with clinical parameters.

Materials and Methods This single-center retrospective analysis included 230 patients (74 female; mean age 63.8 years) with CCTA within 21 months between 01/2018 and 09/2019 without non-pathological examinations. cFFR values were obtained using a deep learning-based non-commercial research prototype (cFFR Version3.5.0; Siemens Healthineers GmbH, Erlangen). cFFR values were evaluated at two points: at the maximum point of the stenosis and 1.0 cm distal to the stenosis. Comparison with invasive coronary angiography in 57/230 patients (24.7 %) was performed. CT parameters and quality were evaluated. Further subgroup classification concerning criteria of technical postprocessing was performed: no changes necessary, minor corrections necessary, major corrections necessary, and no evaluation was possible. The required time from starting the software to the final result was evaluated.

Results A total of 116/448 (25.9 %) mild, 223/448 (49.8 %) moderate, and 109/448 (24.3 %) obstructive stenoses was found. The mean cFFR at the maximum point of the stenosis was 0.92 ± 0.09 and significantly higher than the cFRR value of 0.89 ± 0.13 distal to the stenosis ($p < 0.001^*$). The mean degree of stenosis was 44.02 ± 26.99 % (range: 1–99 %) with an area of 5.39 ± 3.30 mm2. In a total of 45 patients (19.1 %), a relevant reduction in cFFR below 0.80 was determined. Overall, in 57/230 patients (24.8 %), catheter angiography was performed. No significant difference in the degree of maximal stenosis (CAD-RADS 0–2/3/4) was detected between the classification of CCTA and ICA ($p = 0.171$). The mean post-processing time varied significantly with 8.34 ± 4.66 min. in single-vessel CAD vs. 12.91 ± 3.92 min. in two-vessel CAD vs. 21.80 ± 5.94 min. in three-vessel CAD (each $p < 0.001$).

Conclusion Noninvasive onsite quantification of cFFR is feasible with minimal observer interaction in a routine real-world setting on a 128-row scanner. Deep learning-based algorithms allow a robust and semi-automatic on-site determination of cFFR based on data from standard CT scanners.

Key Points:

- Non-invasive on-site quantification of cFFR is feasible with minimal observer interaction.
- Deep-learning based algorithms allow robust and semi-automatic on-site determination of cFFR.
- The mean follow-up time varied significantly with the extent of vascular CAD.

ZUSAMMENFASSUNG

Ziel Implementierung der technischen Machbarkeit von cFFR mittels eines 128-Zeilen-Computertomographen in der alltäglichen Routine. Nachbearbeitung und Alltagstauglichkeit sollen am Gerät vor Ort in Zusammenschau mit klinischen Parametern analysiert werden.

Material und Methoden Diese retrospektive Single-Center-Studie umfasste 230 Patienten (74 weiblich; Durchschnittsalter 63,8 Jahre) mit CCTA innerhalb von 21 Monaten zwischen 01/2018 und 09/2019. Es wurden nur Patienten mit KHK-Befunden eingeschlossen. Die cFFR-Werte wurden mit einem auf Deep Learning basierenden nicht-kommerziellen Forschungsprototyp (cFFR Version3.5.0; Siemens Healthineers GmbH, Erlangen) ermittelt. Die cFFR-Werte wurden an zwei Punkten ausgewertet: am Maximum einer Stenose und 1,0 cm distal der Stenose. Ein Vergleich mit der invasiven Koronarangiographie wurde bei 57/230 Patienten (24,7 %) durchgeführt. Es erfolgte eine weitere Untergruppeneinteilung nach dem Aufwand des Postprocessings: keine Änderungen erforderlich, geringfügige Korrekturen erforderlich, größere Korrekturen erforderlich und keine Auswertung möglich. Bewertet wurde zusätzlich die benötigte Zeit vom Start der Software bis zum Endergebnis.

Ergebnisse Insgesamt wurden 116/448 (25,9 %) leichte, 223/448 (49,8 %) mittelschwere und 109/448 (24,3 %) obstruktive Stenosen gefunden. Der mittlere cFFR-Wert am Maximum der Stenose betrug 0,92 ± 0,09 und war signifikant höher als der cFFR-Wert 0,89 ± 0,13 distal der Stenose ($p < 0{,}001^*$), wobei eine signifikante Korrelation zwischen beiden Werten zu verzeichnen ist ($r = 0{,}966$, $p = 0{,}001^*$). Der mittlere Stenosegrad betrug 44,02 ± 26,99 % (Range 1–99 %) mit einer Fläche von 5,39 ± 3,30 mm2. Bei insgesamt 45 Patienten (19,1 %) wurde eine relevante Verringerung der cFFR unter 0,80 festgestellt. Insgesamt wurde bei 57/230 Patienten (24,8 %) eine Katheterangiographie durchgeführt. Es wurde kein signifikanter Unterschied zwischen dem Grad der maximalen Stenose (CAD-RADS 0–2/3/4) zwischen der Klassifizierung von CCTA und ICA festgestellt ($p = 0{,}171$). Die mittlere Nachbearbeitungszeit zeigte signifikante Unterschiede mit 8,34 ± 4,66 min bei Ein-Gefäß-KHK vs. 12,91 ± 3,92 min bei Zwei-Gefäß-KHK vs. 21,80 ± 5,94 min bei Drei-Gefäß-KHK (jeweils $p < 0{,}001$).

Schlussfolgerung Die nicht-invasive Vor-Ort-Quantifizierung der cFFR ist mit minimaler Nachbearbeitung des Untersuchers im Alltag auf einem 128-Zeilen-Scanner für die cFFR möglich. DL-basierte Algorithmen ermöglichen eine robuste und halbautomatische Vor-Ort-Bestimmung der cFFR auf Daten von Standard-CT-Scannern.

Kernaussagen:

- Die nicht-invasive Vor-Ort-Qunatifizierung der cFFR ist mit minimalem Nachbearbeitungsaufwand möglich.
- Deep-Learning-basierte Algorithmen ermöglichen eine robuste und halbautomatische Bestimmung des cFFR vor Ort.
- Die Nachbearbeitungszeit variiert signifikant je nach Ausmaß der KHK.

Zitierweise

- Baumeister T, Kloth C, Schmidt S et al. On-site CT-derived cFFR in patients with suspected coronary artery disease: Feasibility on a 128-row CT scanner. Fortschr Röntgenstr 2024; 196: 62–71

ABBREVIATIONS

AUC	Area under the curve
BMI	Body mass index
BPM	Beats per minute
CAD	Coronary artery disease
CAD-RADS	Coronary Artery Disease Reporting and Data System
CCTA	Coronary computed tomography angiography
CT	Computed tomography
$_C$FFR	CT-based calculation of fractional flow reserve
ECG	Electrocardiogram
FDA	US Food and Drug Administration
HIPAA	Health Insurance Portability and Accountability Act
ICA	Invasive catheter angiography
LAD	Left anterior descending artery
LCX	Left circumflex artery
MACE	Major cardiac event
NPV	Negative predictive value
PGMI	Perfect, Good, Moderate, Inadequate
PPV	Positive predictive value
RCA	Right coronary artery

Introduction

Coronary artery disease (CAD) is the major cause of mortality and morbidity worldwide. It is challenging for the health care system and its budget [1, 2]. Several noninvasive tests can be used to stratify CAD [3, 4].

Coronary CT angiography (CCTA) is widely accepted as a reliable noninvasive modality for the exclusion of obstructive coronary stenosis [5]. It is a robust diagnostic test to rule out severe coronary

stenosis. However, CCTA has limited specificity in determining the functional significance of coronary stenoses [6–8].

For this reason, its main application is in patients with a low-to-intermediate pre-test risk [9].

CCTA identified many patients with CAD requiring invasive catheter angiography (ICA). However, no significantly obstructed coronary vessels could be identified subsequently [10]. More than 50 % of lesions that appear to be obstructive on CCTA do not cause ischemia [11]. For this reason, the invasive FFR during catheter angiography is considered the gold standard for testing for ischemia [12]. The convincing scientific basis for broad use of the invasive FFR has so far been in strong contrast to the rather limited use in the clinical routine. With the constant technical development of modern computed tomography and the associated post-processing, there is the possibility of computed tomography (CT)-based calculation of the fractional flow reserve $_{C}$FFR. Several studies showed that a $_{C}$FFR value below 0.75–0.80 indicates a relevant stenosis which should be treated by revascularization [13–15]. cFFR using advanced computational analytic approaches allows hemodynamic assessment of a coronary lesion with a single non-invasive test, so that this can be combined with the anatomical information from the CCTA scan [16]. $_{C}$FFR has already been proven to be superior to CCTA in the detection of hemodynamically significant stenoses. It is an independent prognostic risk factor for cardiac events and survival [17, 18]. The technical aspect of the feasibility of $_{C}$FFR has been proven in several multi-center studies, both on the basis of using scanners with at least 64 detector rows and mostly on high-end CT devices [17, 19].

Computational fluid dynamics modeling techniques allow a precise calculation of cFFR noninvasively from standard CCTA images [20]. In this context, the $_{C}$FFR provides superior diagnostic information for the identification of stenoses but has to be further investigated in individual cases and with respect to the degree of severity [21, 22].

Nevertheless, cFFR models are complex and use different information regarding geometric, hemodynamic, and material parameters [23]. To challenge this, on-site machine-learning (ML)-based approaches for calculating cFFR were developed. Currently, the use of investigational artificial intelligence with deep machine learning algorithm software is well established as a potential time-efficient approach [24–26].

The aim of this retrospective single-center study is to evaluate the everyday practicability of the method on the scanner on-site, both in prospectively triggered and retrospectively gated examinations. The analysis not only focusses on comparing diagnostic accuracy with coronary computed tomographic angiography (CCTA) and invasive catheter angiography (ICA) but also encompasses post-processing, as well as technical and formal aspects of implementation, in conjunction with clinical parameters

Material and methods

Study population

In a single-center retrospective analysis of the database of the radiological department, 230 patients (74 female; 156 male, mean age 63.8 ± 9.4 years) with CCTA performed within 21 months between 01/2018 and 09/2019 and pathological findings were identified. The case selection is explained in detail in ▶ **Fig. 1**. Exclusion criteria were coronary anomalies, stents, CT scans with reduced quality (step artifacts, image noise), datasets with software problems, coronary artery aneurysm, chronic obstruction of coronary arteries, and significant stenosis of the main branch.

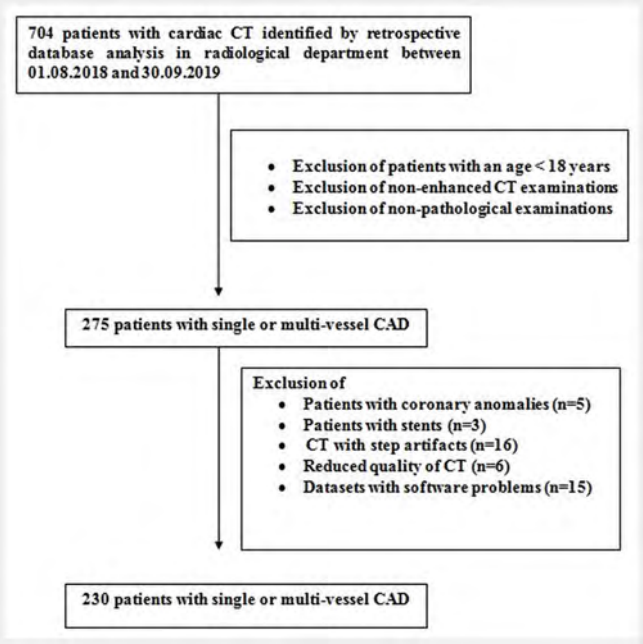

▶ **Fig. 1** Patient recruitment.

CT examinations

CCTA was performed according to the guidelines of the Society of Cardiovascular Computed Tomography. CT examinations were performed on Somatom Definition AS + (Siemens Healthcare GmbH, Erlangen) with a 128-row detector. Image acquisition was prospectively triggered to the patients' electrocardiogram at max. 30 % to 80 % of the R-R interval per our routine clinical practice for CCTA, with a slice thickness of 0.75 mm and a reconstruction increment of 0.5 mm. Either prospective or retrospective electrocardiography synchronization (with X-ray tube current modulation for retrospective electrocardiography-gated protocols) was used for image acquisition. Sublingual nitroglycerin was administered 5 min. prior to scanning in all patients unless a contraindication was present. A beta blocker was given in the case of a heart rate over 65 beats per minute unless a contraindication was present. The maximum beta blocker dose was 100 mg metoprolol tartrate per os or 20 mg metoprolol tartrate i. v. CT examinations included intravenous contrast media injection (Imeron 400, Bracco Imaging Germany) in a weight-adapted dose. Contrast agent was injected at a flow rate of 4–6 mL/sec by antecubital vein. Timing bolus or bolus tracking was used, depending on the protocol.

CT quality was ranked as perfect, good, moderate, or inadequate (PGMI).

Software technique

Analyses of fractional flow reserve from CCTA were performed using a dedicated AI-based research software prototype (cFFR, version 3.5; Siemens Healthcare GmbH, Erlangen) [25, 26]. A patient-specific model of the coronary artery tree was calculated using a semiautomatic approach.

The step-and-shoot procedure (prospective electrocardiogram (ECG) triggering) was used in n = 141 patients (61.3 %) and the helix method (retrospective ECG triggering) in n = 89 patients (38.7 %).

First, centerlines were automatically extracted by the software and had to be accepted by the reader. After acceptance or correction of the luminal contour proposals, a three-dimensional mesh representing the coronary artery tree was calculated.

After correction and acceptance of the coronary tree geometry and the myocardial mass by the user, the software used a multilayer neural network architecture to compute the functional severity of the lesion based on the anatomic information and the calculated hemodynamic conditions [24–26]. By using this semiautomatic on-site software approach, there was only a minimal need for human input.

No side branches were evaluated. $_{C}$FFR values ≤ 0.8 were regarded as significant stenosis. $_{C}$FFR values were evaluated at two points: at the maximum point of the stenosis and 1.0 cm distal to the stenosis. The lesion was identified on the basis of the CCTA finding and the parallel review of the ICA.

The degree of maximal stenosis was categorized according to the CAD-RADS scheme: non-significant stenosis (0–49 % stenosis; CAD-RADS 0–2), moderate stenosis (50–70 %, CAD-RADS 3) and obstructive stenosis (70–99 %, CAD-RADS 4). Vessels with total occlusion (CAD-RADS 5) were excluded because of falsification of the anatomic model of the coronary artery tree.

Furthermore, the Agatston Score, stenosis degree, and stenosis area were evaluated (last two points were shown in supplemental material).

Postprocessing analysis

To assess post-processing, we evaluated the mean post-processing time from starting the patient in the software to the final result of the evaluation.

Additionally, a subgroup classification concerning technical post-processing was performed:

I. No changes necessary (post-processing time < 15 min.)
II. Minor corrections necessary (centerline corrections, post-processing time between 15 and 25 min.)
III. Major correction necessary (post-processing time > 25 min., > 2 corrections, centerline and lumen correction necessary)
IV. Technical failure = no evaluation possible

Furthermore, the required time from starting the software to the final result was evaluated.

Invasive coronary angiography

Invasive coronary angiography was performed as the gold standard. Invasive FFR measurements were obtained in cases of intermediate stenoses or lesions suspicious for coronary artery disease. An FFR value of less than or equal to 0.80 was considered diagnostic for lesion-specific myocardial ischemia. Invasive FFR enrollment was correlated by senior cardiac consultants (BD, BP).

Comparison invasive coronary angiography and $_{C}$FFR values

The cFFR measured for each lesion was compared point by point with the ICA report. Stenosis over 70 % was classified as obstructive according to the CAD-RAD classification. In general, the degree of stenosis was compared, i. e., according to the CAD-RADS scheme. Depending on the evaluation, a correct finding was the confirmation of the exclusion of a relevant CAD or the confirmation of the presence of an obstructive form of the same. The invasive FFR was given to us as a numerical value by the treating cardiologists. Here because of the small number a further evaluation was not performed.

Compliance with ethical standards/ethical approval

This study received no funding. Our local ethics board approved this retrospective study and waived the written informed consent requirement (No. 408/19). All procedures performed in studies involving human participants were in accordance with the ethical standards of the institutional and national research committee and with the 1964 Helsinki declaration and its later amendments or comparable ethical standards. The study was HIPAA compliant.

Statistics

Statistical analysis was performed using dedicated software (IBM SPSS 27.0, Armonk, USA). All results are expressed as mean with standard deviation or median with interquartile ranges. The Kolmogorov-Smirnov test and Shapiro-Wilk test were used for testing normality including Lilliefors significance correction. Paired t-test was used for testing between cFFR values at different levels of the stenosis.

The Kruskal-Wallis test was used for comparison between the different post-processing times.

An invasive FFR of 0.80 or less was the reference standard. Bonferroni adjustment was made for multiple comparisons. The sensitivity, specificity, positive predictive value, and negative predictive values of CCTA, coronary angiography, and cFFR were calculated.

Results

Cohort characteristics

An overview of patient characteristics is given in ▶ **Table 1, 2**. All patient characteristics did not show a normal distribution (height, weight, BMI, diabetes, hypertonus, hypercholesterolemia, smoking, each $p < 0.001^*$). The mean height was 173 cm, the mean weight was 84.25 kg, and the mean BMI was 28.10. Within the subgroup of three-vessel CAD, hypercholesterolemia was significantly higher than in the subgroup of two-vessel CAD ($p < 0.001^*$) and in single-vessel CAD ($p = 0.048^*$). Diabetes was significantly more

▶ **Table 1** Overview of patient characteristics distributed to vessel CAD.
Abbreviations: CAD = coronary artery disease; IQR = interquartile range.

Patient characteristics and risk factors				
	Overall	**Single-vessel CAD**	**Two-vessel CAD**	**Three-vessel CAD**
	n (%)	***n (%)***	***n (%)***	***n (%)***
	230/230(100 %)	115/230 (50.0 %)	67/230 (29.1 %)	58/230 (20.9 %)
Previously known CAD	126/230 (54.7 %)	46/115 (40.0 %)	36/67 (53.7 %)	44/58 (75.9)
Diabetes	31/230 (13.4 %)	13/115 (11.3 %)	7/67 (10.4 %)	11/58 (18.9 %)
Hypertonus	138/230 (60.0 %)	69/115 (60.0 %)	40/67 (59.7 %)	29/58 (50.0 %)
Hypercholesterolemia	76/230 (33.0 %)	34/115 (29.5 %)	18/67 (26.8 %)	24/58 (41.3 %)
Smoking	32/230 (13.9 %)	18/115 (15.6 %)	9/67 (13.4 %)	5/58 (8.6 %)
Agatston Score	328.3 IQR:69.0–617.3	142.2 IQR:16.3–150.3	360.5 IQR:79.4–486.1	731.2 IQR:265.1–1085.5

▶ **Table 2** Overview of patient characteristics distributed to cFFR. Comparison of Agatston values showed a significant difference (p = < 0.001*). However, other characteristics (diabetes, hypertonus, hypercholesterolemia, and smoking) did not show a significant difference (n.s.) tested by chi square post hoc test.

	cFFR< 0.80	**cFFR> 0.80**
	n (%)	***n (%)***
	50/230 (21.7 %)	180/230 (78.3 %)
Diabetes	9/50 (18.0 %)	22/180 (12.2 %)
Hypertonus	31/50 (62.0 %)	107/180 (59.4 %)
Hypercholesterolemia	15/50 (33.3 %)	61/180 (33.9 %)
Smoking	7/50 (14.0 %)	25/180 (13.9 %)
Agatston Score	693.56 IQR:128.89–1330.59	310.62 IQR:67.99–561.98

common in the subgroup of three-vessel CAD than in the subgroup of two-vessel CAD (p = 0.038*).

The three-vessel CAD Agatston score was 731.2 (IQR 265.1–1085.5) and thus significantly higher than in two-vessel CAD with 360.5 (IQR 79.4–486.1) (p < 0.001) and in single-vessel CAD with 142.2 (IQR: 16.3–150.3) (p < 0.001). The correlation between Agatston Score and distal FFR is shown in ▶ **Fig. 2** (r = 0.046 p < 0.001*).

There were a total of 116/448 (25.9 %) mild, 223/448 (49.8 %) moderate, and 109/448 (24.3 %) obstructive stenoses. Of these, 91/448 (20.3 %) were located in the RCA, 96/448 (21.4 %) in the LCX, and 261/448 (58.3 %) in the LAD.

CT parameter/quality

CT datasets with inadequate quality (n = 2) were excluded before statistical analysis. 32/230 (13.9 %) datasets had perfect quality, 122/230 (53.0 %) had good quality, and 74/230 (32.2 %) had moderate quality. 89/230 (38.7 %) CT scans were acquired retrospectively, 141/230 (61.3 %) prospectively.

The mean overall heart rate per minute was 60.5 ± 9.5 bpm (min. heart rate 55.4 ± 8.8 bpm, max. heart rate 67.9 ± 19.4 bpm). The RR distance was 1009.5 ± 140.0 ms.

In the subgroup of prospectively acquired CT scans, the mean heart rate was 58.3 ± 6.9 bpm vs. in the subgroups of retrospectively acquired CTs 64.6 ± 11.9 bpm, p = 0.001*. The min. heart rate of prospectively acquired CT scans was 54.4 ± 6.6 bpm, which was significantly lower than in the retrospectively acquired scans (58.0 ± 11.1 bpm), p = 0.010*. The max. heart rate showed no significant difference (66.9 ± 24.1 bpm vs. 72.8 ± 19.7 bpm, p = 0.054). The RR distance was significantly lower in the subgroup of prospectively acquired CT scans with 948.8 ± 158.0 ms vs. 1033.3 ± 116.1 ms (p = 0.001*).

$_C$FFR values and correlation with invasive catheter angiography

The mean $_C$FFR at the maximum point of the stenosis was 0.92 ± 0.09 and was significantly higher than the $_C$FFR value of 0.89 ± 0.13 distal to the stenosis (p < 0.001*). A significant correlation between the two values was registered (r = 0.966, p = 0.001*). An example is given in ▶ **Fig. 3**.

A detailed overview of stenosis parameters is given in **supplemental material Table 1**.

Overall, in 57/230 patients (24.7 %), a catheter angiography examination was performed, while an invasive measurement of FFR was performed in only 2/48 patients. In ICA, more than one lesion was not suspected to be hemodynamically relevant with a necessity for FFR measurement in any patient.

No significant difference was detected between the degree of maximal stenosis (CAD-RADS 0–2/3/4) in CCTA and ICA (p = 0.171).

Overall, the degree of stenosis in CCTA correlated significantly with the degree of stenosis in ICA (r = 0.076, p < 0.001*). In subgroups of single-vessel CAD, it did not correlate significantly

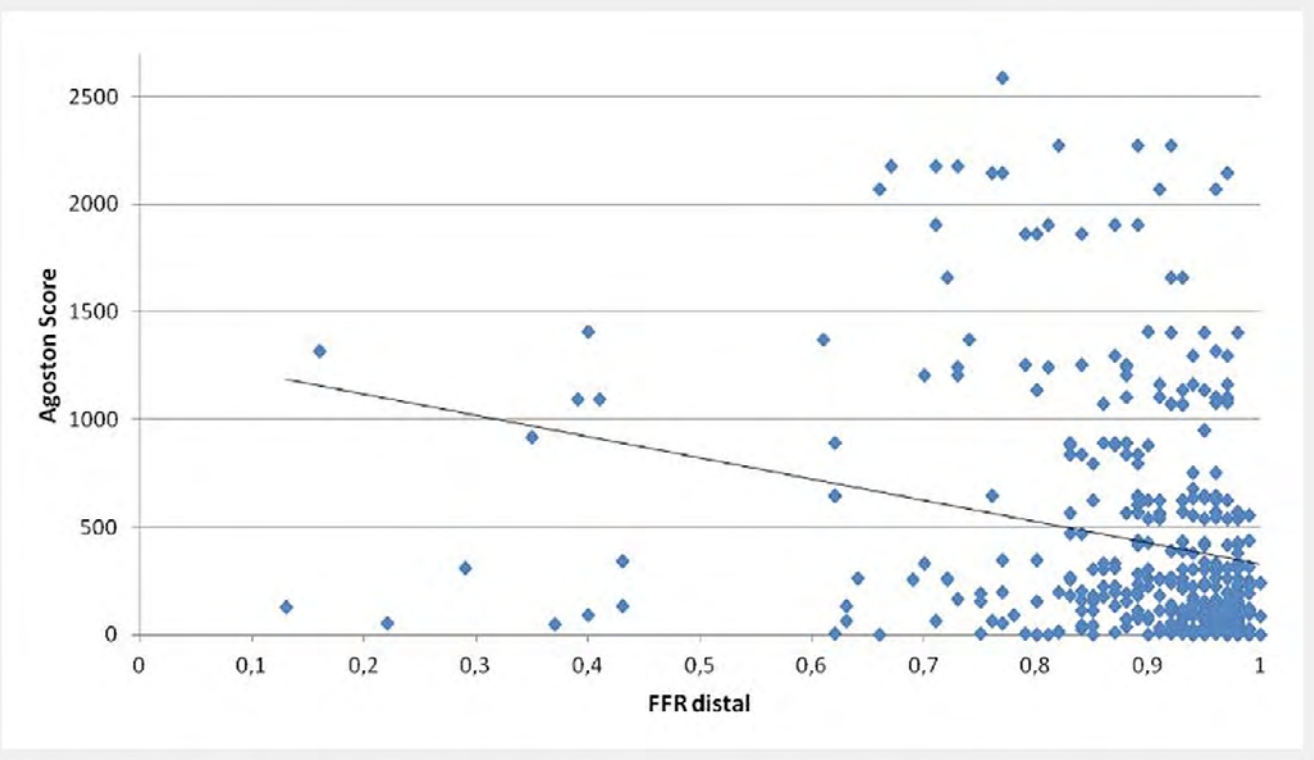

▶ **Fig. 2** Correlation of Agatston score with cFFR distal to the stenosis (r = 0.046, p < 0.001*).

(r = 0.162, p = 0.092). However, a low significant correlation could be registered in two- and three-vessel CAD (r = 0.122, p < 0.001*/ r = 0.126 p < 0.001*).

Overall, the $_{C}$FFR values correlated significantly with the degree of stenosis in ICA (distal r = 0,084, p < 0.001*, at maximum point of stenosis r = 0,08, p = 0.003*).

Univariate linear regression analyses are additionally given in ▶ **Table 3**.

Sensitivity/specificity/positive predictive value/ negative predictive value

With a combination of CCTA and cFFR, a per vessel sensitivity/specificity/PPV/NPV of 70.6 %, 67.7 %, 64.3 %, and 73.7 %, respectively, were achieved. The detailed results are given in **supplemental material Tables 2–4**.

Postprocessing analysis

Additionally, a subgroup classification concerning technical postprocessing was performed. An overview is given in ▶ **Table 4**.

A significant, but weak correlation between the increasing subgroup and the number of vessels in CAD was registered (r = 0.041, p < 0.001*), also with $_{C}$FFR values (r = 0.061, p < 0.001*). In contrast to this, no significant correlations could be registered between the degree of stenosis in CCTA and patient characteristics (height, weight, BMI, diabetes, hypertonus, hypercholesterolemia, smoking, each p = ns). The rejection rate was 16.3 % with 45 rejected examinations, e. g., for inadequate image quality.

Post-processing time

Significantly different mean postprocessing times were registered with 8.34 ± 4.66 min. in single-vessel CAD vs. 12.91 ± 3.92 min. in two-vessel CAD vs. 21.80 ± 5.94 min. in three-vessel CAD (each p < 0.001*). An overview is given in ▶ **Fig. 4**.

The range in men is significantly greater than in women. In particular, the range of times required is greater in men with three-vessel CAD, but there is no significant difference between men and women in the three subgroups (p = 0.506, p = 0.433 and p = 0.219, respectively for single/two/three-vessel CAD).

Discussion

This study demonstrates the technical feasibility of semiautomatic on-site software for $_{C}$FFR in the daily routine on a 128-row CT scanner with minimal human input and corrections. A specificity of 82.3 % for $_{C}$FFR could be achieved and a significant increase in sensitivity was achieved by combining $_{C}$FFR and CCTA compared to a sensitivity of $_{C}$FFR alone (70.6 % vs. 31.4 %). Our results also show that a measurement 1.0 cm distal to the stenosis is suitable for precise detection of $_{C}$FFR values.

The diagnostic performance of $_{C}$FFR has been validated in several major studies, both for the HeartFlow technique and for a research prototype by *Siemens Healthineers GmbH* [27–29]. A $_{C}$FFR value < 0.8 was the cut-off level for lesion-specific ischemia and shows a good correlation between $_{C}$FFR and invasive FFR. Catheter-based invasive fractional flow reserve still tends to be used, and with technical progress and artificial intelligence, $_{C}$FFR meas-

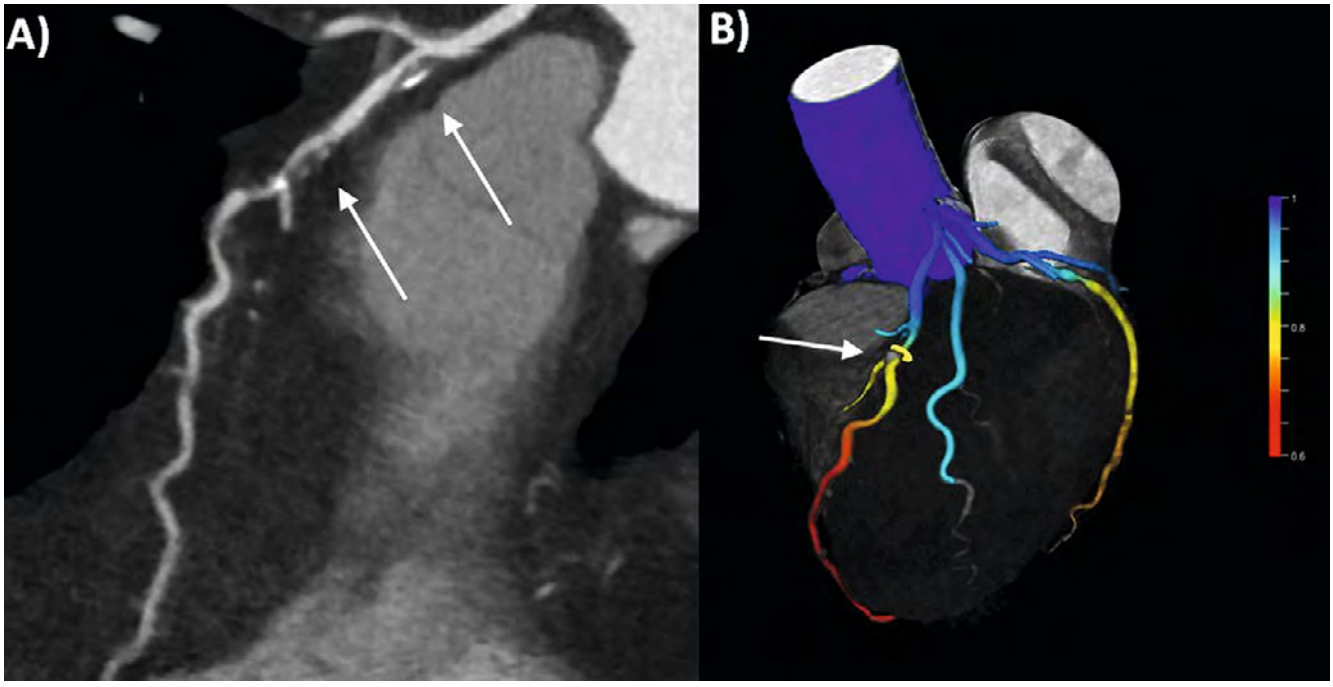

▶ **Fig. 3** Evaluation of a 60-year-old male patient with two-vessel CAD. The patient underwent CCTA for the evaluation of coronary status; in CCTA, multiple significant stenoses were detected in LAD (A) and in the proximal LCX. By evaluating the cFFR, significant stenosis can be verified: values of 0.72 and 0.64 were evaluated at the proximal stenosis and 1.0 cm above (B). In LCX complementary values of 0.79 and 0.72 were evaluated. One month after CCTA, the patient underwent invasive catheter angiography with quadruple stent supply of the LAD.

▶ **Table 3** Univariate linear regression analyses for predictors of cFFR (distal). A p-value < 0.05 was considered statistically significant.

cFFR (distal) and	r^2	p-value
Degree of stenosis in CCTA	r = 0.180	p < 0.001*
Degree of stenosis in ICA	r = 0.41	p = 0.018*
Agatston Score	r = 0.051	p < 0.001*
Post-processing time	r = 0.012	p = 0.011*
cFFR proximal	r = 0.924	p < 0.001*

urement was tested as an on-site approach [27]. Although there is evidence supporting their clinical use, $_C$FFR techniques are not routinely applied in each patient up to now in clinical practice [30]. Here our study proved the feasibility in everyday use with minimal observer interaction in a routine real-world setting on a standard 128-row CT scanner.

1. Patient characteristics

Within the subgroup with three-vessel CAD, the prevalence of hypercholesterolemia and diabetes was significantly higher than in the other subgroups. Diabetes and hypercholesteremia are known risk factors for the development of CAD and damage to the small vessels in particular. These results are in line with the study by Zhu X. et al in 2022, who showed that the percentage of patients with a history of diabetes is higher in subgroups with major cardiac events (MACE) (70.9 % vs. 66.3 %, p < 0.05) [31]. Xue Y et al. showed that diabetes has no negative impact on the diagnostic accuracy of machine learning–based $_C$FFR [32]. Especially patients with type two diabetes mellitus have a high burden of CAD already in an early stage of the disease, and an advantage from hemodynamic evaluation of significant CAD by $_C$FFR is proven [33].

2. $_C$FFR evaluation

The $_C$FFR was significantly higher at the maximum point of stenosis than distal to the stenosis. These results are in line with the studies by Nozaki Y. et al and Kueh S. et al., who showed that a $_C$FFR measured 1–2 cm distal to a target stenosis is more consistent with the decision for revascularization than measured at the maximum point of the stenosis [34, 35].

Similarly, in invasive FFR, ischemia evaluation is typically performed by establishing the ratio of the coronary pressure within 1–2 cm distal to an anatomical stenosis and pressure at the level of the aorta at maximal hyperemia [35].

Overall, the degree of stenosis in CCTA and the $_C$FFR values correlated significantly with the degree of stenosis in ICA. This is consistent with the results of two large studies (DeFACTO and NXT), where the investigators demonstrated the superiority of $_C$FFR with a good correlation between $_C$FFR and invasive FFR [27, 36].

Overall and concordant to the literature, CCTA showed a strong negative predictive value and a specificity up to 72.5 %, which is a little less than in other current single-center studies

▶ **Table 4** Overview of post-processing analysis classification distributed to vessel CAD. Additionally, a subgroup classification concerning criteria of technical post-processing was performed.

	I	II	III	IV	Overall
	No changes necessary	**Minor corrections necessary**	**Major correction necessary**	**Technical failure, no evaluation possible**	
Single-vessel CAD	72	37	7	0	115
Two-vessel CAD	6	36	24	0	66
Three-vessel CAD	1	17	28	2	49
	79	90	59	2	230

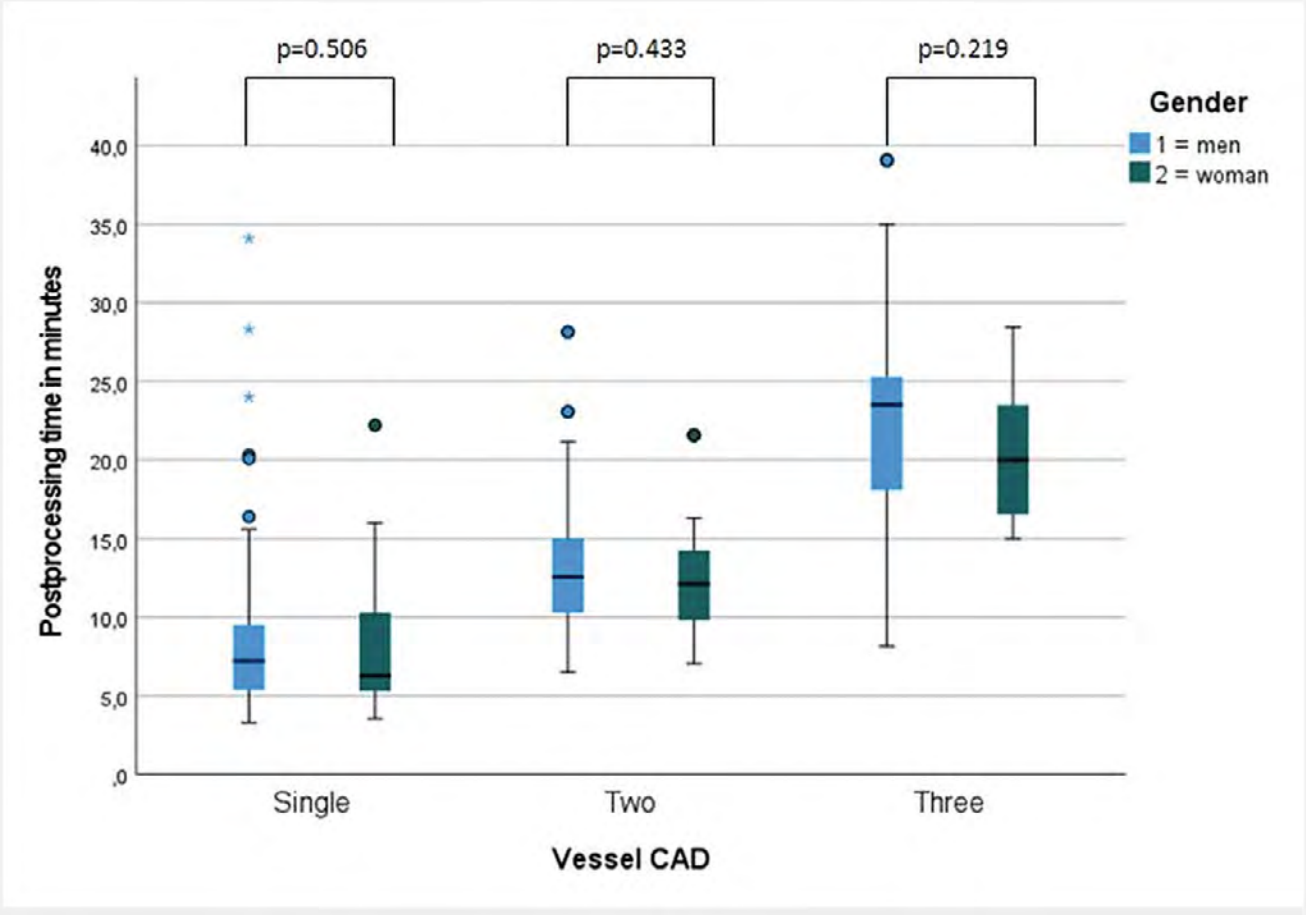

▶ **Fig. 4** Distribution of post-processing time in minutes compared to vessel CAD and gender. The scatter in men is significantly greater than in women. In particular, the range of times required is greater among men with three-vessel CAD, but there is no significant difference between men and women in the three subgroups (p = 0.506; p = 0.433, and p = 0.219, respectively, for single/two/three-vessel CAD).

[37, 38]. Chua A. et al showed a sensitivity of 75.1 % in a comparable Australian collective [38]. The cFFR results were slightly below average compared to other current studies with a specificity of 82.3 % and a sensitivity of 31.4 %. The lower results are most likely due to the group of patients who received invasive angiography as the gold standard. On the one hand, due to the location, patients with relevant suspicion of significant CAD receive direct ICA. On the other hand, the patients we saw only received secondary angiography in the case of unclear CT findings. A systematic correlation by means of catheter angiography does not take place due to the location, so that the collective is more inhomogeneous compared to prospectively planned studies. Another reason can be the relatively high overall Agatston Score in the patient collective, which could have a negative effect on the accuracy of the

$_C$FFR. The diagnostic performance of the recently introduced machine-learning algorithm still requires further investigation [40].

The mean overall Agatston Score in our study was 330.2 ± 488.8. Mickley H et al. already showed that most patients with an Agatston Score > 399 had at least one stenosis with a cFFR ≤ 0.80 [39]. Tesche et al. showed also a high performance in low-to-intermediate Agatston scores (0 to 400) with a statistically significant difference (AUC 0.71 vs. 0.85, p = 0.04) [40].

Hamilton et al. showed that in "real-world" practice $_C$FFR does not improve standard radiological assessment of coronary disease graded by CAD-RADS alone [41]. In their analysis of 1145 coronary CT examinations the use of $_C$FFR in CAD-RADS 2–4 resulted in reduced accuracy and specificity without a significant increase in sensitivity [41]. $_C$FFR reduced the accuracy of the CAD-RADS grade significantly from 91 % to 78.4 % in their study [41].

3. CT parameter/quality

At 16.3 % the rejection rate in our study was equal to or slightly lower than in other single-center study in the current literature where it ranges from 13 % to 33 % [2, 27]. The main reason for $_C$FFR rejection in our study was motion artifacts, as in the study by Pontone G. et al. [2].

Additionally, a novel subgroup classification concerning criteria of technical postprocessing was established. A significant correlation between the degree of necessary post-processing steps and the degree of CAD was registered.

The time required for post-processing increased significantly with the degree of CAD (each $p < 0.001^*$). As expected, the post-processing effort is greater in patients with multivessel CAD than in patients with only single lesions. In patients with 3-vessel CAD, the processing time increased significantly, so that in this patient group with a high pre-test probability of a relevant stenosis, the use of cFFR must be critically questioned. The overall time consumption of post-processing is little less than other single-center studies.

4. Limitations

There are several limitations to this study. First, not all patients underwent invasive catheter angiography and only a minute number underwent an additional invasive FFR. This might be due to the clinical stage of CAD in the included patients.

Second, the applied cFFR software prototype in this study is not FDA-approved compared to other commercial applications. Third, no side branches of the coronaries were evaluated. Fourth, the evaluation of cFFR and CCTA was not performed double-blinded, and the reader of the cFFR dataset knew the CCTA results in each case. Fifth, the cFFR evaluation was only performed with one software/vendor. A comparison to the HeartFlow software solution was not performed, which limited the significance of the results regarding daily practice. Six, it is a single-center study with patients from a circumscribed spatial area. There is a selection bias with respect to patients and CT quality. Seventh, tandem stenoses were not explicitly excluded. These are included in the description statistics because they were included in the original CCTA assessment.

Conclusion

Noninvasive on-site quantification of $_C$FFR is feasible with acceptable observer interaction in a routine real-world setting on a 128-row scanner. DL-based algorithms allow a robust and semi-automatic on-site determination of $_C$FFR using data from standard CT scanners.

Conflict of Interest

C. Panknin is an employee of Siemens Healthcare. None of the authors have conflicts of interest to be stated. No grants or other forms of financial support were utilized for this work.

References

[1] Lucas FL, DeLorenzo MA, Siewers AE et al. Temporal trends in the utilization of diagnostic testing and treatments for cardiovascular disease in the United States, 1993-2001. Circulation 2006; 113 (3): 374–379

[2] Pontone G, WeirMcCall JR, Baggiano A et al. Determinants of rejection rate for coronary CT angiography fractional flow reserve analysis. Radiology 2019; 292 (3): 597–605

[3] Miller JM, Rochitte CE, Dewey M et al. Diagnostic performance of coronary angiography by 64-row CT. N Engl J Med 2008; 359 (22): 2324–2336

[4] Meijboom WB, Meijs MFL, Schuijf JD et al. Diagnostic Accuracy of 64-Slice Computed Tomography Coronary Angiography. A Prospective, Multicenter, Multivendor Study. J Am Coll Cardiol 2008; 52 (25): 2135–2144

[5] Li Y, Yu M, Dai X et al. Detection of hemodynamically significant coronary stenosis: CT Myocardial Perfusion versus Machine Learning CT Fractional Flow Reserve. Radiology 2019; 293 (2): 305–314

[6] Chang HJ, Lin FY, Lee SE et al. Coronary Atherosclerotic Precursors of Acute Coronary Syndromes. J Am Coll Cardiol 2018; 71 (22): 2511–2522

[7] Mori H, Torii S, Kutyna M et al. Coronary Artery Calcification and its Progression: What Does it Really Mean? JACC: Cardiovascular Imaging 2018; 11 (1): 127–142

[8] Van Rosendael AR, Narula J, Lin FY et al. Association of High-Density Calcified 1K Plaque with Risk of Acute Coronary Syndrome. JAMA Cardiology 2020; 5 (3): 282–290

[9] Zhuang B, Wang S, Zhao S et al. Computed tomography angiography-derived fractional flow reserve (CT-FFR) for the detection of myocardial ischemia with invasive fractional flow reserve as reference: systematic review and meta-analysis. Eur Radiol 2020; 30 (2): 712–725

[10] Asher A, Singhal A, Thornton G et al. FFRCT derived from computed tomography angiography: the experience in the UK. Expert Review of Cardiovascular Therapy 2018; 16 (12): 919–929

[11] Min JK, Taylor CA, Achenbach S et al. Noninvasive Fractional Flow Reserve Derived From Coronary CT Angiography: Clinical Data and Scientific Principles. JACC: Cardiovascular Imaging 2015; 8 (10): 1209–1222

[12] Xaplanteris P, Fournier S, Pijls NHJ et al. Five-year outcomes with PCI guided by fractional flow reserve. N Engl J Med 2018; 379 (3): 250–259

[13] De Bruyne B, Pijls NHJ, Kalesan B et al. Fractional flow reserve-guided PCI versus medical therapy in stable coronary disease. N Engl J Med 2012; 367 (11): 991–1001

[14] Gassenmaier S, Tsiflikas I, Greulich S et al. Prevalence of pathological FFRCT values without coronary artery stenosis in an asymptomatic marathon runner cohort. Eur Radiol 2021; 31 (12): 8975–8982

[15] Tonino PAL, De Bruyne B, Pijls NHJ et al. Fractional flow reserve versus angiography for guiding percutaneous coronary intervention. N Engl J Med 2009; 360 (3): 213–224

[16] Tesche C, Cecco CND, Albrecht MH et al. Coronary CT Angiography-derived Fractional Flow Reserve. Radiology 2017; 285 (1): 17–33. doi:10.1148/radiol.2017162641

[17] Ihdayhid AR, Norgaard BL, Gaur S et al. Prognostic value and risk continuum of noninvasive fractional flow reserve derived from coronary CT angiography. Radiology 2019; 292 (2): 343–351

[18] Lu MT, Ferencik M, Roberts RS et al. Noninvasive FFR Derived From Coronary CT Angiography: Management and Outcomes in the PROMISE Trial. JACC: Cardiovasc Imaging 2017; 10 (11): 1350–1358

[19] Shi K, Yang FF, Si N et al. Effect of 320-row CT reconstruction technology on fractional flow reserve derived from coronary CT angiography based on machine learning: single- versus multiple-cardiac periodic images. Quant Imaging Med Surg 2022; 12 (6): 3092–3103. doi:10.21037/qims-21-659

[20] Lu MT, Ferencik M, Roberts RS et al. Noninvasive FFR Derived From Coronary CT Angiography: Management and Outcomes in the PROMISE Trial. JACC: Cardiovascular Imaging 2017; 10 (11): 1350–1358

[21] Koo BK, Erglis A, Doh JH et al. Diagnosis of ischemia-causing coronary stenoses by noninvasive fractional flow reserve computed from coronary computed tomographic angiograms: Results from the prospective multicenter DISCOVER-FLOW (Diagnosis of Ischemia-Causing Stenoses Obtained Via Noninvasive Fractional Flow Reserve) study. J Am Coll Cardiol 2011; 58 (19): 1989–1997

[22] Min JK, Leipsic J, Pencina MJ et al. Diagnostic accuracy of fractional flow reserve from anatomic CT angiography. JAMA – Journal of the American Medical Association 2012; 308 (12): 1237–1245

[23] Dey D, Lin A. Machine-Learning CT-FFR and Extensive Coronary Calcium: Overcoming the Achilles Heel of Coronary Computed Tomography Angiography. Jacc: Cardiovascular Imaging 2020; 13 (3): 771–773

[24] Martin SS, Mastrodicasa D, van Assen M et al. Value of Machine Learning–based Coronary CT Fractional Flow Reserve Applied to Triple-Rule-Out CT Angiography in Acute Chest Pain. Radiology: Cardiothoracic Imaging 2020; 2 (3): e190137

[25] Tesche C, De Cecco CN, Baumann S et al. Coronary CT angiography-derived fractional flow reserve: Machine learning algorithm versus computational fluid dynamics modeling. Radiology 2018; 288 (1): 64–72

[26] Coenen A, Lubbers MM, Kurata A et al. Fractional flow reserve computed from noninvasive CT angiography data: Diagnostic performance of an on-site clinicianoperated computational fluid dynamics algorithm. Radiology 2014; 274 (3): 674–683

[27] Norgaard BL, Leipsic J, Gaur S et al. Diagnostic performance of noninvasive fractional flow reserve derived from coronary computed tomography angiography in suspected coronary artery disease: The NXT trial (Analysis of Coronary Blood Flow Using CT Angiography: Next Steps). J Am Coll Cardiol 2014; 63 (12): 1145–1155

[28] Nakanishi R, Matsumoto S, Alani A et al. Diagnostic performance of transluminal attenuation gradient and fractional flow reserve by coronary computed tomographic angiography (FFR(CT)) compared to invasive FFR: a sub-group analysis from the DISCOVER-FLOW and DeFACTO studies. The International Journal of Cardiovascular Imaging 2015; 31 (6): 1251–1259

[29] Raja J, Seitz MP, Yedlapati N et al. Can Computed Fractional Flow Reserve Coronary CT Angiography (FFRCT) Offer an Accurate Noninvasive Comparison to Invasive Coronary Angiography (ICA)? "The Noninvasive CATH." A Comprehensive Review. Curr Probl Cardiol 2021; 46 (3): 100642

[30] Coenen A, Rossi A, Lubbers MM et al. Integrating CT Myocardial Perfusion and CT-FFR in the Work-Up of Coronary Artery Disease. Jacc: Cardiovascular Imaging 2017; 10 (7): 760–770

[31] Zhu X, Pang Z, Jiang W et al. Synergistic prognostic value of coronary distensibility index and fractional flow reserve based cCTA for major adverse cardiac events in patients with Coronary artery disease. BMC Cardiovascular Disorders 2022; 22 (1): 220

[32] Xue Y, Zheng MW, Hou Y et al. Influence of diabetes mellitus on the diagnostic performance of machine learning-based coronary CT angiography-derived fractional flow reserve: a multicenter study. Eur Radiol 2022; 32 (6): 3778–3789

[33] Mrgan M, Norgaard BL, Dey D et al. Coronary flow impairment in asymptomatic patients with early stage type-2 diabetes: Detection by FFR_{CT}. Diabetes & Vascular Disease Research 2020; 17 (9): 1479164120958422

[34] Nozaki YO, Fujimoto S, Kawaguchi YO et al. Prognostic value of the optimal measurement location of on-site CT-derived fractional flow reserve. J Cardiol 2022; 80 (1): 14–21

[35] Kueh SH, Mooney J, Ohana M et al. Fractional flow reserve derived from coronary computed tomography angiography reclassification rate using value distal to lesion compared to lowest value. Journal of cardiovascular computed tomography 2017; 11 (6): 462–467

[36] Yun C, Hung C, Wen M et al. CT Assessment of Myocardial Perfusion and Fractional Flow Reserve in Coronary Artery Disease: A Review of Current Clinical Evidence and Recent Developments. Korean Journal of Radiology 2021; 22 (11): 1749–1763

[37] Gao Y, Zhao N, Song L et al. Diagnostic Performance of CT FFR With a New Parameter Optimized Computational Fluid Dynamics Algorithm From the CT-FFR-CHINA Trial: Characteristic Analysis of Gray Zone Lesions and Misdiagnosed Lesions. Frontiers in Cardiovascular Medicine 2022; 9: 819460

[38] Chua A, Ihdayhid A, Linde JJ et al. Diagnostic Performance of CT-Derived Fractional Flow Reserve in Australian Patients Referred for Invasive Coronary Angiography. Heart, Lung & Circulation 2022; 31 (8): 1102–1109

[39] Mickley H, Veien KT, Gerke O et al. Diagnostic and Clinical Value of FFR_{CT} in Stable Chest Pain Patients With Extensive Coronary Calcification: The FACC Study. Jacc: Cardiovascular Imaging 2022; 15 (6): 1046–1058

[40] Tesche C, Otani K, De Cecco CN et al. Influence of Coronary Calcium on Diagnostic Performance of Machine Learning CT-FFR: Results From MACHINE Registry. Jacc: Cardiovascular Imaging 2020; 13 (3): 760–770

[41] Hamilton MCK, Charters PFP, Lyen S et al. Computed tomography-derived fractional flow reserve (FFRCT) has no additional clinical impact over the anatomical Coronary Artery Disease – Reporting and Data System (CAD-RADS) in real-world elective healthcare of coronary artery disease. Clin Radiol 2022. doi:10.1016/j.crad.2022.05.031